

# Numerical comparison between the Dynamic mode decomposition and the Arnoldi extraction technique on an afterburner test case

Guillaume Jourdain\*, Lars-Erik Eriksson†

The fairly recent methodology, the so called Dynamic Mode Decomposition, is investigated for the Afterburner test case in order to see if the methodology is able to capture thermo-acoustic instabilities. Previous papers<sup>9,10,11</sup> deal with the prediction of such instabilities using the Arnoldi extraction technique. The present paper compares these two approaches in order to see their advantages and drawbacks regarding the present case of study. The linearized solver chosen in the Arnoldi extraction technique is based on the Linearized Navier Stokes Equations (LNSE). As a main concern of the study, the structures and frequencies of the buzz ( $\sim 120$  Hz) and the screech modes ( $\sim 1200$  Hz) are compared using both methodologies. Additional cases are also studied acoustic liner walls in computational domain and tuned to damp the Screech mode. In these cases the methodologies are tested for their ability to predict the damping effect of the liner.

## Nomenclature

### *Latin symbols*

$A$	Matrix of the system analyzed in the Dynamic mode decomposition
$A_{Arn}$	Matrix of the system analyzed in the Arnoldi extraction method
$B^{Kry}$	Orthonormal base of Krylov subspace
$E_i$	Pseudo-eigenvector
$N_{step}$	Number of time steps
$P$	Perturbation field, vector

### *Greek symbols*

$\Delta t$	Time step
$\lambda^A$	Eigenvalue computed in the Arnoldi extraction method
$\lambda_i$	Eigenvalue computed in the Dynamic mode decomposition
$\xi$	Damping factor

### *Superscript*

*	Hermitian operator
---	--------------------

### *Abbreviations*

CAA	Computational Aero-Acoustics
CFD	Computational Fluid Dynamics
DMD	Dynamic Mode Decomposition
HAP	High Amplitude Perturbation
$K_{ss}$	Krylov subspace
LAP	Low Amplitude Perturbation
LNSE	Linearized Navier-Stokes Equations
URANS	Unsteady Reynolds Averaged Navier-Stokes Equations

---

\*Graduate Student, Department of Applied Mechanics, Chalmers University of Technology, Sweden

†Professor, Department of Applied Mechanics, Chalmers University of Technology, Sweden

## I. Introduction

COMBUSTION instabilities occur often in confined chambers. A typical example of a combustion chamber is a combustor in a gas turbine. Inside the combustor pressure oscillations may couple with the heat release generated by the combustion<sup>1</sup>. Simple changes in the settings of a few physical parameters can move the combustion from a stable regime to an unstable one. Instability is undesirable since it can lead to major damage in the gasturbine. Usually thermo-acoustic instabilities are damped by performing some postdesign which firstly is very costly and secondly could lead to modification of the overall characteristics of the combustor.

A numerical tool has thus been developed in order to be able to analyze the stability of a combustor. The tool is based on Computation Fluid Dynamics (CFD) and Computational Aero-Acoustics (CAA) together with an Arnoldi extraction technique<sup>8,9</sup>. The key idea is that thermo-acoustic instabilities evolve above a mean flow field since they involve acoustic waves. Therefore the CFD has for main purpose to solve mean flow field while acoustic waves are solved using in the present case a linear solver<sup>2,3</sup>, here the LNSE solver<sup>7,10</sup> based on the Linearized Navier Stokes Equations. To be able to distinguish modes of oscillations by their frequencies the Arnoldi extraction technique based on the same linear solver (LNSE) is used. As a result it generates a wealth of modes where each of them has its own structure containing acoustic and/or hydrodynamic waves and its own frequency.

A new approach, the so called Dynamic Mode Decomposition<sup>12</sup> (DMD), considered as an Arnoldi-like method, was developed in order to analyze nonlinear problems using empirical data. The set of data that depicts a field, in the present case, a flow field, at different times but with the same time interval (snapshots). The Dynamic Mode Decomposition is built on a linear model that links the snapshots of the flow field in order to compute eigenvalues and eigenvectors that capture the main features of the dynamic processes occurring in the flow field. Each eigenvalue and its corresponding eigenvector represent a mode which is frequency-fixed, contains coherent structures and has a growing/damping rate. These characteristics make the new approach as suitable as the Arnoldi extraction technique to analyze thermo-acoustic instabilities.

To understand in practice similarities and differences between the two methodologies a test case is chosen: the so called Validation Rig I. This atmospheric test rig is divided in two parts, the first to premix propane/air and the second to ignite the gas mixture at the flameholder in the combustor part. The test rig was run at Volvo Aero Corporation between 1990 – 1992<sup>4,5,6</sup> and has the advantage to contain experimental data. Moreover numerical analyses using the Arnoldi extraction technique is also available for the test rig. The remaining information required is the numerical analyses of the test rig using DMD which is presented in the following paragraphs. Inside the test rig two unstable modes may occur, these are the so called buzz ( $\sim 120\text{ Hz}$ ) and screech ( $\sim 1200\text{ Hz}$ ) modes. In order to validate the extraction technique, e.g. based on Arnoldi or DMD, these two modes have to be captured and this is thus a criterion when comparing both approaches.

## II. Methodologies

The Arnoldi and DMD methodologies require both the initial use of a URANS solver. The solver used here is based on an in-house code called G2DNAV that relies on the full Navier-Stokes equation for unsteady compressible flow, including a two-equation turbulence model (realizable k-epsilon model). The numerical method used in the solver is the finite volume method and the meshes are of multiblock-structured type. The convective and diffusive fluxes are computed by a 3rd-order upwind biased scheme and a 2nd order compact centered scheme respectively. The time stepping is achieved with an explicit three stage Runge-Kutta algorithm<sup>7</sup>. The combustion model is a single-step global mechanism together with a slightly modified Magnussen-Hjertager model (1976) which takes into account the effect of the turbulence on the reaction rates. A porous wall model is also used for the liner modeling and it is built on recently published work<sup>11</sup> where the non-linear as well as inertial effects are taken into account.

## A. The Arnoldi based approach

The CAA method that follows on the Arnoldi based approach<sup>8</sup> relies on an LNSE solver. This solver is built on the Linearized Navier-Stokes Equations which means that viscous terms are taken in account even the turbulent eddy viscosity. The eddy viscosity of the mean flow is assumed to be fixed in time and thus considered as a frozen field. The strategy behind the use of the frozen eddy viscosity approach comes from the fact that k-epsilon source terms are highly non-linear and thus not suitable for a linearized approach. The combustion model is also excluded from the linearized solver since it is partly based on the turbulent quantities  $k$  and  $\varepsilon$ . The baseline of the linearization is the previously described URANS solver.

Starting from an initial "rich" perturbation plus the data regarding the mean flow, the algorithm based on the Arnoldi method computes the evolution of the initial perturbation for a specific number of time steps. The initial "rich" perturbation is computed by the LNSE solver from a "crude" initial perturbation which excites practically all possible modes. After a large number of LNSE time steps the crude perturbation becomes smoother and the field contains mainly the least damped modes. This field is the initial "rich" perturbation  $P_1$  for the algorithm based on the Arnoldi method. Assuming that the evolution of perturbation field  $P_i$  can be described by a matrix  $A_{Arn}$ , the perturbations fields  $P_1$  to  $P_n$  can be expressed as in 1.

$$P_2 = A_{Arn}P_1 \text{ and } P_{i+1} = A_{Arn}P_i \text{ where } i = 1 \dots n-1 \quad (1)$$

The Krylov subspace  $K_{ss}$  spanned by the perturbation fields  $P_1 \dots P_m$  can be described by an orthonormal base  $B^{Kry} = [b_1^{Kry}, \dots, b_m^{Kry}]$ . This base  $B^{Kry}$  is built by the Arnoldi algorithm as in 2.

$$\left[ \begin{array}{l} \text{Initialisation and normalisation of the first vector of basis } b_1 \\ b_1^{Kry} = \frac{P_1}{\sqrt{(P_1)^T P_1}} \text{ where } ^T \text{ is the transpose operator} \\ \text{Computation of orthogonalized vector } P_{k+1}^{or} \text{ for } k = 1 \text{ to } m-1 \\ P_{k+1}^{or} = A_{Arn}b_k^{Kry} - \sum_{l=1}^k h_{l,k}b_l^{Kry} \\ \text{where } h_{l,k} \text{ are coefficients for a } m \times m \text{ upper Hessenberg matrix } H^m \\ \text{and are defined as } h_{l,k} = (b_l^{Kry})^T A_{Arn}b_k^{Kry} \\ \text{Computation of vector's norm } P_{k+1}^{or} : h_{k+1,k} = \sqrt{(P_{k+1}^{or})^T P_{k+1}^{or}} \\ \text{Normalisation of the vector } P_{k+1}^{or} : b_{k+1}^{Kry} = \frac{P_{k+1}^{or}}{h_{k+1,k}} \end{array} \right. \quad (2)$$

By performing the previous algorithm, the Hessenberg matrix  $H_m$  can be directly related to the matrix  $A_{Arn}$  as in 3

$$H_m = B^{Kry*} A_{Arn} B^{Kry} \quad (3)$$

where  $*$  denotes the Hermitian operator. An eigendecomposition is then performed on the upper Hessenberg matrix  $H_m$  as in 4.

$$H_m V_i^A = \lambda_i^A V_i^A \quad (4)$$

By rearranging equation 4 and combine it with 3, the eigenvalues  $\lambda_i^A$  and eigenvectors  $V_i^A$  of the matrix  $B^{Kry*} A_{Arn} B^{Kry}$  are computed as shown in 5. They represent the eigenvalues and eigenvectors of the projection of the matrix  $A_{Arn}$  on the Krylov subspace and they modes of fluctuations for fixed frequencies.  $B^{Kry} V_i^A$  are then defined as  $E_i^A$  and are the pseudo-eigenvectors of  $A_{Arn}$  since they obtained by the eigendecomposition of the projection  $A_{Arn}$  on the Krylov subspace.

$$\begin{aligned} H_m V_i^A &= B^{Kry*} A B^{Kry} V_i^A \\ B^{Kry} \lambda_i^A V_i^A &= A_{Arn} B^{Kry} V_i^A \\ B^{Kry*} (A_{Arn} (B^{Kry} V_i^A) - \lambda_i^A (B^{Kry} V_i^A)) &= 0 \end{aligned} \quad (5)$$

## B. Dynamic Mode Decomposition

The Dynamic Mode Decomposition<sup>12</sup> is a fairly recent method where the data obtained by experiments and/or CFD can be used to recover a matrix  $A$  that describes the system of equations that the set of data obeys. We start with a data set

$$V_m \equiv [v_1, \dots, v_m] \quad (6)$$

where  $v_1 \dots, v_m$  represent snapshots of the flow field with dimension  $n$ . The Single Value Decomposition algorithm is applied to the matrix  $V_m$

$$V_m = U\Sigma W^* \text{ with } U, W \text{ orthonormal matrices of sizes } (n,n) \text{ and } (m,m) \quad (7)$$

where  $\Sigma$  a diagonal matrix of size  $(n,m)$ . Assuming a linear relationship between  $V_m$ , the  $m$  first snapshots and  $V_{m+1} \equiv [v_2, \dots, v_{m+1}]$  containing  $m$  snapshots of the flow field but from the second one to  $m+1$ , expression (8) is obtained.  $A$  represents the matrix describing the evolution of the system, in the present paper the equations that the fluid obeys. Expression 7 is now inserted into equation 8, to obtain the projection of  $A$  as in expression 9. The system is projected by introducing the pseudo-inverse of the diagonal matrix  $\Sigma$ ,  $\Sigma^{-1}$  which is diagonal matrix of a size  $(m,m)$  containing the quadratic part of  $\Sigma$  and the matrix  $U_m$  of size  $(n,m)$  and which defined as the first  $m$  columns of  $U$ .

$$V_{m+1} = AV_m \quad (8)$$

$$\begin{aligned} V_{m+1} &= AU\Sigma W^* \\ V_{m+1}W\Sigma^{-1} &= AU_m \\ U_m^* V_{m+1}W\Sigma^{-1} &= U_m^* AU_m \end{aligned} \quad (9)$$

Here  $U_m^* AU_m$  represents the matrix  $A$  which theoretically contains the physical laws obeyed by considered system projected on the subspace spanned by  $V_m$ . The next step is to perform an eigendecomposition of the projected matrix  $U^*AU$  in order to computed the potential modes of oscillations of the flow field in the specified domain.

$$\begin{aligned} U_m^* AU_m Z_i &= \lambda_i Z_i \\ U_m^* V_{m+1} W \Sigma^{-1} Z_i &= \lambda_i Z_i \end{aligned} \quad (10)$$

where  $\lambda_i$  and  $Z_i$  are eigenvalues and eigenvectors of the  $(m,m)$  matrix  $U^*AU$ . One of the important advantages of the method is revealed with equation 10 above. There is no need to know the matrix  $A$  describing the physical laws of the systems. The only information required are the snapshots of instantaneous solutions of flow field and a constant time interval between them.

$$\begin{aligned} AU_m Z_i &= \lambda_i U_m Z_i \\ AE_i^{DMD} &= \lambda_i E_i^{DMD} \end{aligned} \quad (11)$$

where  $E_i^{DMD}$  defined as  $U_m Z_i$  are the pseudo-eigenvectors of the matrix  $A$ , pseudo-eigenvectors since they were obtained in 12 by the projection  $U_m^* AU_m$ . Since  $A$  was computed using only the snapshots computed by the URANS solver but the linear analysis itself was not built onto a CFD solver. That is a main difference between the Arnoldi procedure based on the LNSE solver and the Dynamic mode decomposition. Here there is no need to develop and to use a linear solver like the LNSE solver. One of the constraints of LNSE solver is the assumption that the turbulence flow field is frozen and that the combustion is excluded for the investigation of the modes of oscillations. The combustion feedback generated by modes of oscillation is thus not included in the Arnoldi based approach. In the Dynamic mode decomposition approach the combustion feedback information is embedded in the snapshots. Furthermore the Dynamic mode decomposition can be performed by using only one physical variable while the Arnoldi extraction method requires all degrees of freedom to be performed. Reducing the data sets to one variable like the pressure or the density saves significantly the CPU time.

There are nevertheless similarities in both approaches. First of all a perturbation has to be generated in the flow field and the evolution of this perturbation should be computed for several time steps before recording the snapshots of the instantaneous flow field. This procedure is required so that only physically relevant modes of oscillations remain in the computational domain. By saving the snapshots too early the physical modes could be polluted by very shortlived modes. Similarly by saving the snapshots too late after the initiation of the perturbation the modes of oscillations may be too drowned by round-off errors to be extracted. The generation of a perturbation field, rich in physical modes of oscillations, faces the same

limits as in the Arnoldi procedure. On top of that the flow field could also be non stationary meaning for instance that oscillations occur naturally around a mean flow field that only exists by averaging a number of snapshots. Such natural oscillations (limit cycles) occur in the presented cases. In such a case the snapshots contain both oscillations generated by the initial perturbation plus the natural oscillations.

The DMD can also be performed using different data set when using the same test case. The initial data basis  $V_m$  can actually contain either (1) directly the snapshots obtained from the URANS computations or (2) the fluctuations in these snapshots by subtracting a mean solution or (3) by defining each vector column in the matrix  $V_m$  as the difference between two following snapshots. In the present study, the method (2) and (3) have been performed.

### C. Frequencies and Damping

For either Arnoldi extraction method or Dynamic Mode Decomposition, the frequencies and the damping coefficients are computed in the same fashion as shown below:

$$\begin{aligned} \text{Arg}(\lambda) &= 2\pi f N_{step} \Delta t + 2\pi p \\ \xi &= \frac{\ln|\lambda|}{N_{step} \Delta t} \end{aligned} \quad (12)$$

where  $\lambda$  is an eigenvalue either obtained by the DMD based or the Arnoldi based approach,  $N_{step}$  is the number of time step between each snapshot for DMD or each computation of a Krylov orthonormal vector for Arnoldi,  $\Delta t$  is the time step and  $p$  is an integer. The damping factor has nevertheless a difference in their interpretation. The damping factor  $\xi$  does take into account the coupling between the acoustic waves and the heat release fluctuations when the Dynamic mode Decomposition is used to extract modes. The same damping coefficient takes only into account the aerodynamical damping for the modes extracted using the Arnoldi based approach.

## III. Geometry of the Rig

The experimental Validation Rig is divided into two parts (Figure 1). The inlet part, 0.55 m long, ensures the mixing of the propane, with the air. Air enters the rig at the inlet via a choked plate while the fuel is released into the rig 0.15 m downstream via choked fuel injectors. Both parts have a rectangular cross area which is 0.12 meter high and 0.24 meter wide. The inlet part contains as well several honeycomb/screens. The second part of the rig is the combustor part where the mixture is ignited behind a flameholder. The flameholder is characterized by its cross section which is an equilateral triangle with an edge of 4 cm and by its location, 0.318 m downstream of the inlet of the combustor part. The combustor part which is one meter long ends by a sudden expansion which multiplies the cross section area by 3.4.

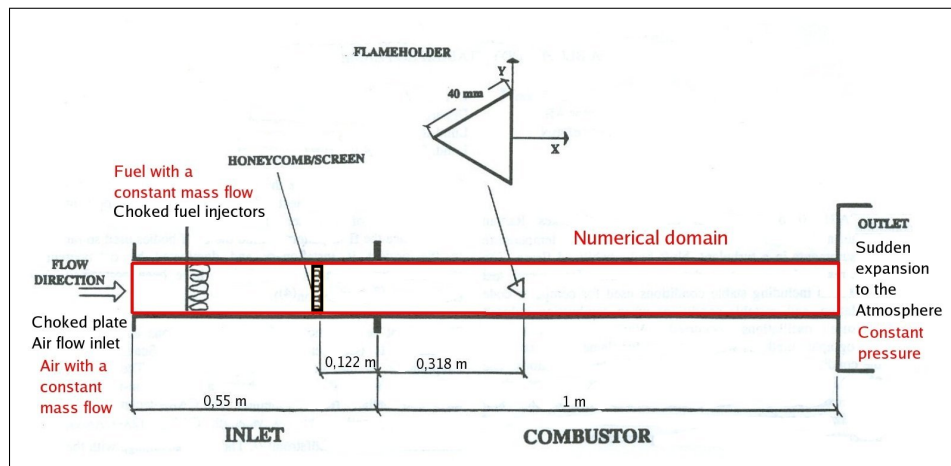


Figure 1. Geometry of the Validation Rig I

## IV. Computational grid

The computational grid (Figure 2) is divided into four regions. Three include the test rig while the fourth is a "virtual region" as long as the validation rig and 2 *cm* wide between the red (solid walls) and green walls. This region is "open" when solid walls are locally replaced by porous walls (walls in green). In such a case, the porous walls start 10 *cm* upstream the flameholder and end 20 *cm* downstream. The number of cells in the domain is around 30000.

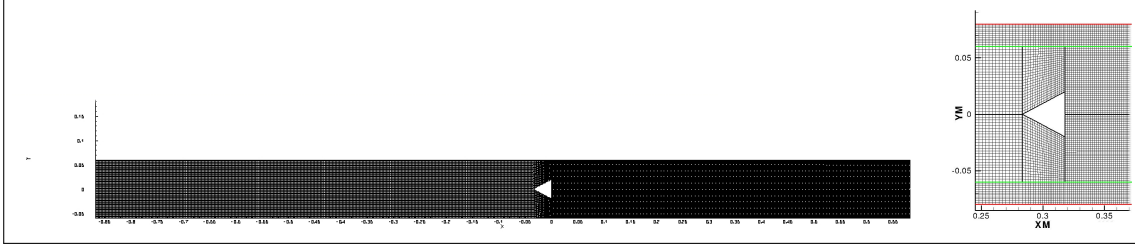


Figure 2. Computational grid and enlargement of the grid in flameholder region. The green color represents solid walls than can be changed into porous walls. The red color represents solid walls

## V. Experimental and Numerical Boundary conditions

The numerical domain follows the same geometry as the described one above but is adapted to be modeled in 2D. The mass flow is 1.1 kg/s, the temperature of the unburned mixture in the inlet part is 288 K and the equivalence ratio  $\phi$  is 0.72 as in the experiment. The experimental rig has solid walls at its boundaries except at the inlet and the outlet. That is also the case for the numerical domain nevertheless the numerical domain has been as well slightly modified to include porous walls for specific cases. The porous wall is tuned so that the liner resonance frequency is 1200 Hz. The linear resistance of the porous wall is assumed to be  $10Ns/m^3$ . It is worth noticing that a previous investigation showed that the linear resistance of the porous wall did not affect significantly the damping of the resonance frequency<sup>11</sup>. Two different amplitudes of perturbations are applied to the flow field before performing the Dynamic mode decomposition. In both cases, the perturbation is generated at the inlet of the computation domain. The URANS solver is first run for 200 time steps with the chosen perturbation set at the inlet. The inlet boundary conditions are then set back to their normal values and the URANS solver is run for 10000 time steps. The key idea is that then the perturbation has reached the flameholder. The snapshots are finally computed and stored after the 10000 time steps run. For the Low Amplitude Perturbation (LAP) the inlet velocity is risen by 3.2 %. Meantime the High Amplitude Perturbation (HAP) is generated by multiplying the inlet velocity by 50 %. The mass flow and the total enthalpy are recomputed to adapt to this change in velocity.

Case	Method	Perturbation	Porous Walls
1	Arnoldi		No
2	DMD	LAP	No
3	DMD	HAP	No
4	Arnoldi		Yes
5	DMD	LAP	Yes
6	DMD	HAP	Yes

Table 1. Description of the test cases

## VI. The buzz and the screech modes

The Validation rig data is of interest since experiments were run for unstable regimes when the buzz and screech modes were encountered. The buzz mode has a frequency of  $120\text{ Hz}$  and can be described as flame flapping phenomenon where fluctuations in the heat release leads to an increase of the size of the "bubble" of burned gases behind the flameholder as shown figure 3. This bubble is nevertheless constrained by the walls of the domain and this generates a reduction of the length of the flame front meaning a reduction of the heat release. The pressure in the bubble decreases and the bubble collapses on itself. The flame front is then long enough to generate a large heat release and a new bubble grows. The screech mode has a frequency of  $1200\text{ Hz}$  and can be described as an interaction between the flame front and vortices. The flame front waves due to this interaction as shown Figure 3.

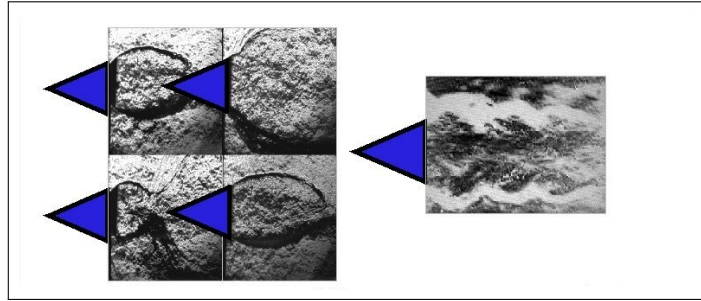


Figure 3. Schlieren pictures, Buzz mode (on the left side) and Screech mode (on the right side) phenomena

## VII. Numerical Results

### A. General comments on extracted modes

The Arnoldi extraction is performed by building a Krylov subspace spanned by 200 vectors. The number of time steps between the computation of a new vector is 1000. The Dynamic mode decomposition is performed using 633 snapshots. The time interval between two snapshots is 100 time steps. The time step chosen for both the Arnoldi extraction method and the Dynamic mode decomposition is  $8 \cdot 10^{-7}\text{ s}$ . Both approaches provide a wealth of different modes of oscillations. There are longitudinal mixed typed modes for low frequencies and transversal mixed typed modes for high frequencies. Previous work has shown that for this test rig transversal modes have too high frequencies to be unstable<sup>4,5,6</sup>. The first transversal mode has a frequency of  $2700\text{ Hz}$ <sup>9</sup>. The study is therefore focused on the differences between screech and buzz mode candidates for the different cases.

### B. Screech mode candidates

For both the Arnoldi extraction method and the Dynamic mode decomposition, candidates for the screech mode is a longitudinal mixed mode as shown in Figures 4, 5. Mixed type modes can be explained by the fact that acoustic pressure waves spread upstream into the rig and generate hydrodynamic waves when they hit the flameholder. These hydrodynamic waves travel downstream and generate acoustic waves when they reach the outlet. The modes have the same structure using either the Arnoldi extraction method or the Dynamic mode decomposition and the frequency range of these screech mode candidates is between  $1132\text{ Hz}$  and  $1182\text{ Hz}$  which is close to the experimental frequency  $1200\text{ Hz}$ .

The Dynamic mode decomposition is then able to capture the screech mode candidates. Furthermore while introducing an extra damping in the case 4 with the use of porous wall, the Arnoldi mode extraction revealed that the screech mode couldn't be captured. This indicated that as the damping of the eigenvalue associated to the screech mode candidate was too high for this mode to be extracted (large negative damping factor  $\xi$ ). The Dynamic mode decomposition shows that screech mode can be extracted even if the porous wall is incorporated into the computation domain as shown in Figure 5. Moreover it appears that the structure of the screech mode is also not affected the damping generated by the porous walls. The ability

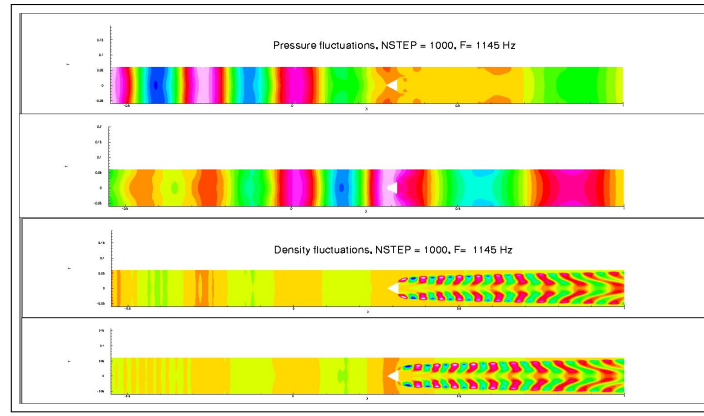


**Figure 4.** Screech candidate obtained by the Arnoldi extraction method based on the LNSE solver (case 1), Pressure and Density fields (real and imaginary parts)

of the Dynamic mode decomposition to extract the screech mode candidate for the cases including porous wall can be explained by the fact that the combustion feedback is included. The relevance of the combustion feedback appears clear while looking at damping factors in the Table 2.

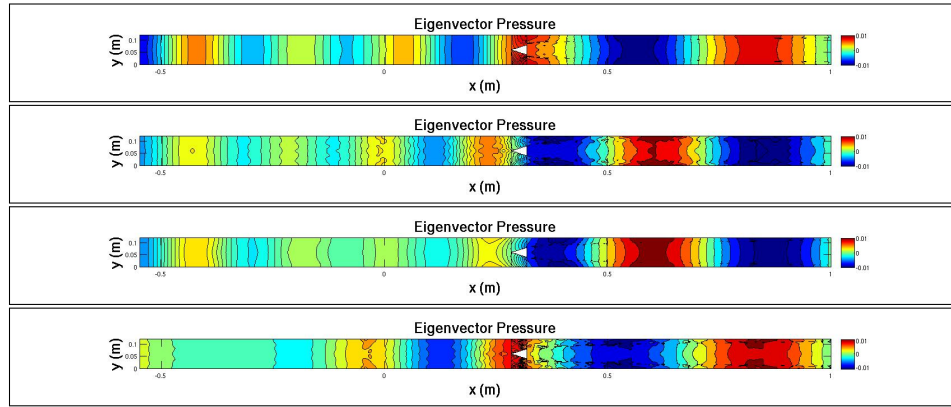


**Figure 5.** Screech candidates obtained by DMD, Pressure fields (real parts). From top to bottom: cases 2 ( $f = 1136 \text{ Hz}$ ) and 3 ( $f = 1176 \text{ Hz}$ ) including only solid walls, and cases 5 ( $f = 1132 \text{ Hz}$ ) and 6 ( $f = 1182 \text{ Hz}$ ) including porous walls

The case 1 is a screech mode candidate given by the Arnoldi extraction method. Its shape is similar to the candidates found using the Dynamic mode decomposition but the damping factor is lower than those computed with the Dynamic mode decomposition for case 2 and 3 respectively  $-103.5 \text{ s}^{-1}$ ,  $8.2 \text{ s}^{-1}$  and  $53.8 \text{ s}^{-1}$ . The combustion feedback acts on the pressure waves and transfers a part of the energy of combustion into these waves. This explains why the damping factor is higher for cases 2 and 3. For the cases 2 and 3 the damping factor is even positive meaning that Screech mode candidate is unstable. These results should be interpreted with some caution. Several modes extracted have frequencies close to screech mode candidate and some have negative damping factors. An energy transfer due to non-linear effects between all these modes could easily happen. Cases 2 and 3 reveal at least that non-linear effects and combustion are important in the computation of the stability of a mode.

The cases 5 and 6 become then interesting when we compare them with the cases 2 and 3 since they show the ability of the acoustic linear to damp some modes of oscillations. In the presented cases the porous wall was tuned to give a maximum damping at  $f = 1200 \text{ Hz}$ . For the cases 2 and 5 the screech mode is extracted using as an initial perturbation, the LAP and the damping factors are  $8.2 \text{ s}^{-1}$  and  $-13.7 \text{ s}^{-1}$  respectively. When the high amplitude perturbation is used as the initial perturbation, the damping factor is also reducing from  $53.8 \text{ s}^{-1}$  for the case 3 to  $-84.2 \text{ s}^{-1}$  for the case 6. For both cases, 5 and 6, the damping



factor is reduced in comparison with its corresponding cases 2 and 3. The porous walls have an effect on the stability on screech mode candidates and this can be achieved for a range of different modes if the porous walls are tuned in this purpose.

Case	frequency (Hz)	$\xi$ ( $s^{-1}$ )
1	1144	-103.5
2	1136	8.2
3	1176	53.8
4	Not captured	
5	1132	-13.7
6	1182	-84.2

**Table 2.** Screech modes candidates for each cases

### C. Buzz mode candidates

The buzz mode candidates found by either the Arnoldi eigenmode extraction or the Dynamic mode decomposition techniques are longitudinal mixed typed modes. The buzz mode candidates have nevertheless different frequencies. For the buzz mode candidate extracted by the Arnoldi method (case 1) the frequency is  $89 \text{ Hz}$  (Figure 6) which is fairly low in comparison with the experimental frequency  $120 \text{ Hz}$ . For the buzz mode candidates extracted by the Dynamic mode decomposition, frequencies are closer to the experimental one, respectively  $135 \text{ Hz}$  for the case 2 and  $125 \text{ Hz}$  for case 3 (Figure 7). One explanation for this improvement in the frequencies of the buzz mode candidates can be once more non-linear effects and the coupling between the pressure oscillations and the heat release fluctuations.

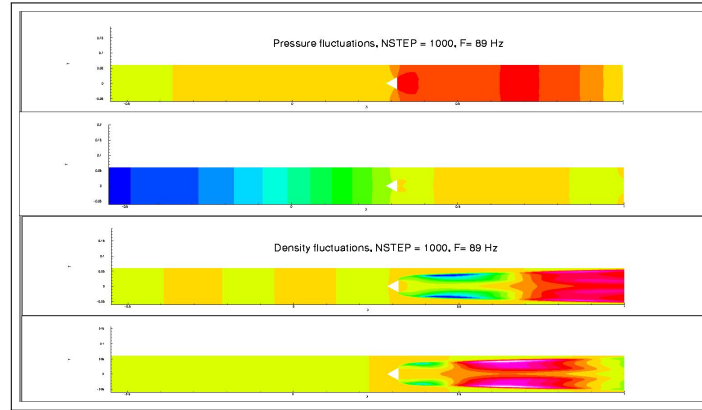


**Figure 6.** Buzz candidates obtained by the Arnoldi extraction method, cases 1 (upper figure,  $f = 89 \text{ Hz}$ ), Pressure and Density fields (real and imaginary parts)

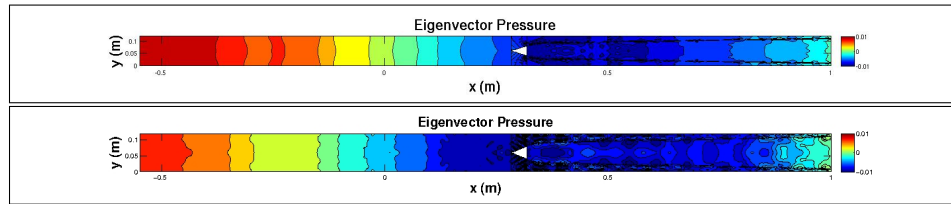


**Figure 7.** Buzz candidates obtained by DMD, cases 2 (upper figure,  $f = 135 \text{ Hz}$ ) and 3 (lower figure,  $f = 125 \text{ Hz}$ ), Pressure fields (real parts)

## VIII. Conclusions

Two different methodologies, the Arnoldi extraction method based on the LNSE solver and the Dynamic mode decomposition based only on the URANS solver, have been investigated in their abilities to capture and describe modes of oscillation in a test rig modeling an afterburner: The Validation Rig I. The Dynamic mode decomposition offers a number of advantages in comparison with the Arnoldi extraction method. First of all the modes can be extracted without the use of any linearized solver. Since a linearized solver, here the LNSE solver, has to be derived and implemented this saves a lot of time and effort. Furthermore linearization enforces two major assumptions: the turbulence is frozen while performing the linear analysis and the combustion model which partly relies on the turbulent quantities  $k$  and  $\epsilon$  has to be excluded. Conversely the Dynamic mode decomposition relies entirely on a set of snapshots obtained by a CFD computation, here a URANS solver based on the realizable  $k$ - $\epsilon$  turbulence model. There is no need to linearize any solver. Another major difference is the fact that the Arnoldi extraction method requires that all degrees of freedom to extract the modes. In the Dynamic mode decomposition the amount of variables can be chosen. Choosing only one variable for instance pressure or density will save much CPU time. From a result perspective, both methods work in the sense that modes of oscillations can be extracted for a wide range of frequencies from tens of  $Hz$  to several  $kHz$ . Two main structures exist for these modes. They are either longitudinal mixed type modes or transversal mixed type modes. The results regarding the study of the buzz and screech modes and the influence of the liner walls are summarized as follows:

1. The screech mode candidate
  - has frequency close to the experimental one  $1200\ Hz$  and is a longitudinal mixed type mode,
  - extracted by the Arnoldi extraction method based on the LNSE solver has a negative damping factor,
  - extracted by the Dynamic mode decomposition based on the URANS solver has a positive damping factor since the combustion feedback is embedded in the snapshots.
2. The buzz mode candidate
  - is a longitudinal mixed type mode,
  - has frequency closer to the experimental one  $120\ Hz$  for modes extracted by the Dynamic mode decomposition based on the URANS solver than the mode extracted by the Arnoldi extraction method based on the LNSE solver. Non-linear effects and the coupling between the pressure oscillations and the heat release fluctuations can be at the origin of the frequency shift.
3. The liner walls tuned to give a maximum damping at  $1200\ Hz$  reveal their ability to decrease the damping factors of the screech mode candidates.

The Arnoldi extraction method and the Dynamic mode decomposition are similar in some aspects but the Dynamic method decomposition has a number of advantages. It contains more physics since it is based on a URANS solver. It can save a lot of CPU time since it is variable selective and it can compute the stability of particular thermo-acoustic modes in the afterburner within the limits given by the turbulence and combustion modeling used.

## IX. Acknowledgments

The research has been funded by the Swedish Energy Agency, Siemens Industrial Turbomachinery AB and Volvo Aero Corporation through the Swedish research program TURBOPOWER, the support of which is gratefully acknowledged. This work is performed at the Department of Applied Mechanics, Division of Fluid Dynamics at Chalmers University of Technology.

## X. References

1. Huang, Y., and Yang, V., "Dynamics and stability of lean-premixed swirl-stabilized combustion", Progress in Energy and Combustion Science, 35 (2009), pp. 293-364.

2. Eriksson, L.-E., Andersson, L., Lindblad, K., Andersson, N., "Development of a Cooled Radial Flameholder for the F404/RM12 Afterburner: Part III Afterburner Rumble Prediction and Suppression", paper ISABE-2003-1060, presented at the 16th ISABE Conf, Cleveland Ohio, September 2003.
3. Eriksson, L.-E., Moradnia, P., "Computational Study of Mixed Hydrodynamic-Acoustic Waves in Gas Turbine Afterburner Flows", paper AIAA-2950, proc. of 14th AIAA/CEAS Aeroacoustics Conf, 5-7 May 2008, Vancouver, Canada.
4. Sjunnesson, A., Olovsson, S., Sjöblom, B., "Validation Rig - A tool for flame studies", presented at 10th ISABE Conf., Nottingham, UK, September 1-6, 1991.
5. Sjunnesson, A., Nelsson, C., Max, E., "LDA measurements of velocities and turbulence in a bluff body stabilized flame", Proc. of 4th International Conf. on Laser Anemometry - Advances and Applications, ASME; Cleveland, August 1991.
6. Sjunnesson, A., Henrikson, P., CARS measurements and visualizations of reacting flows in a bluff body stabilized flame", AIAA-92-3650, presented at 28th Joint Propulsion Conference and Exhibit, Nashville, Tennessee, July 6-8, 1992.
7. Billson, M., Eriksson, L.-E., Davidson, L., "Acoustic source terms for the linear Euler equations on conservative form", AIAA Journal, 43 (4), 2005, pp. 752-759.
8. Saad, Y. "Variations on Arnoldi's method for coupling eigenelements of large unsymmetric matrices", Linear Algebra, and its applications 34: 269-2985, 1980.
9. Jourdain, G. Eriksson, L.-E. "Analysis of thermo-acoustic properties of Combustors and Afterburners", GT2010-22339, proc. ASME Turbo Expo 2010, June 14-18, 2010, Glasgow, UK.
10. Jourdain, G. Eriksson, L.-E. "Combustor stability analysis based on linearized flow solvers and Arnoldi-based eigenmode extraction techniques", AIAA-2010-3866, proc. 16<sup>th</sup> AIAA/CEAS aero-acoustics conference 2010, June 7-9, 2010, Stockholm, Sweden.
11. Jourdain, G. Eriksson, L.-E. "Time-domain modeling of Screech-Damping Liners in Combustor and Afterburners", ISABE-2011-1113, proc. 20<sup>th</sup> ISABE conference 2011, June 12-16, 2011, Gothenburg, Sweden.
12. Chen, Kevin K. Tu, Jonathan H. Rowley, Clarence W. "Variants of dynamic mode decomposition: connections between Koopman and Fourier analyses", Journal of Nonlinear Science, May 25, 2011, Princeton, USA. <http://cwrowley.princeton.edu/publications.php>